Structural Engineering and Mechanics, *Vol. 72, No. 4 (2019) 433-441*
DOI: https://doi.org/10.12989/sem.2019.72.4.433

Nonlinear static analysis of laminated composite beams under hygro-thermal effect

Şeref D. Akbaş*

Department of Civil Engineering, Bursa Technical University, Yıldırım Campus, Yıldırım, Bursa 16330, Turkey

(Received April 2, 2019, Revised May 9, 2019, Accepted June 20, 2019)

Abstract. In this paper, geometrically nonlinear static analysis of laminated composite beams is investigated under hygrothermal effect. In the solution of problem, the finite element method is used within the first shear beam theory. Total Lagrangian approach is used nonlinear kinematic model. The geometrically nonlinear formulations are developed for the laminated beams with hygro-thermal effects. In the nonlinear solution of the problem, the Newton-Raphson method is used with incremental displacement. In order to verify of obtained formulations, a comparison study is performed. The effects of the fiber orientation angles, the stacking sequence of laminates, temperature rising and moisture changes on the nonlinear static displacements and configurations of the composite laminated beam are investigated in the numerical results.

Keywords: hygro-thermal effect; nonlinear analysis; laminated composite beams; total lagragian; finite element method

1. Introduction

Laminated composites have been used a lot of structural systems such as spacecrafts, aircrafts, high thermal systems. Hygrothermal or moisture effects have very important role in the mechanic behavior of laminated composites. After a certain moisture value, the laminated composites can be lost their strength. The design of laminated composite structural elements in the high hygrothermal environments is very important problem. In high temperature and moisture values, large bending deflections can be occurred in the laminated composite structures. It is known that large bending deflections problems are the nonlinear problems. Hence, understanding the nonlinear behavior of laminated composite structure is very important in high hygrothermal values.

There are a lot of studies in linear analysis of laminated composite beams under mechanical and thermal loads in literature. On the other hand, nonlinear studies of laminated composite beams are not investigated broadly. In literature, investigations of hgyrothermal effect in the laminated composite structures are as follows; Cardoso *et al*. (2009) investigated geometrically nonlinear behavior of the laminated composite thin-walled beam structures with finite element solution. Ghayesh *et al*. (2010) presented vibration and stability analysis of axially traveling laminated beams. Rath and Sahu (2010) investigated static and post-buckling analysis of woven laminated composite structures under hygrothermal loading. Zhan *et al*. (2011) presented hygrothermal static behavior of laminated composites with open hole. Sahu *et al*. (2012) and Biswal *et al*. (2016) investigated instability and parametric resonance of curved laminated shell panels under hygrothermal effects. Gayen and Roy (2013) presented hydrothermal effects on the stress distribution of a tapered laminated beam. Zenkour *et al*. (2014) investigated hygrothermal analysis of laminated cross-ply plates. Wang *et al*. (2015) studied dynamic and buckling investigations of laminated plates under hygrothermal effects. Akbaş (2017a,2017b) investigated effects of the thermal loading on the dynamic and static responses of functionally graded porous beams. Bouazza *et al*. (2014) investigated hygrothermal postbuckling behavior of laminated beams based on Von Karman nonlinearity. Li and Qiao (2015) investigated nonlinear postbuckling analysis of composite laminated beams. Ghayesh *et al*. (2017, 2018), Farokhi *et al*. (2017), Kazemirad *et al*. (2013) analyzed nonlinear dynamic responses of laminated and composite beams. Akbaş (2019a) analyzed effects of the hygro-thermal rising on the post-buckling results of the laminated beams. Joshan *et al*. (2017) proposed a new non-polynomial shear deformation theory for hygrothermal analysis of laminated plates. Akbaş (2018a, b, c) investigated nonlinear static deflections and post-buckling responses of laminated composite beams under different loads. Gholami *et al*. (2017) investigated nonlinear dynamic analysis of functionally graded carbon-nanotube reinforced beams based on higher beam theory. Akbaş (2018d,2019b,2019c) presented nonlinear behavior of fiber reinforced composite beams with intact and cracked cases. Akbaş (2019d) presented hygro-thermal nonlinear static results of a functionally graded cantilever beam by using Total Lagrangian nonlinear approach. Ebrahimi and Dabbagh (2018) studied wave propagation of double-layered graphane sheets under hygro-thermal effects.

It seen from literature, the nonlinear hygrothermal studies of laminated composite beams have not been studied in large. Also, the total Lagrangian nonlinear approach has

*Corresponding author, Ph.D.
E-mail: serefda@yahoo.com

ISSN: 1225-4568 (Print), 1598-6217 (Online)

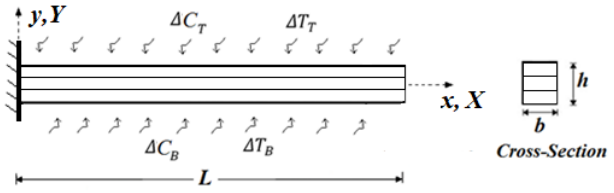

Fig. 1 A cantilever laminated beam under non-uniform moisture and temperature rising

not been used in hygro-thermal analysis of laminated beams. The objective of presented paper is to fill this blank for laminated composite beams. The novelty in this paper is to investigate the nonlinear static displacements of laminated composite beams under hygro-thermal effects by using the total Lagrangian nonlinearity. The finite element method and first shear beam theory are used in solution of problem. The Newton-Raphson approach is utilized in nonlinear solution. The effects of the fiber orientation angles, the stacking sequence of laminates, temperature and moisture rising on the nonlinear static results of laminated composite beams are investigated. Also, a comparison study is presented.

2. Theory and formulation

A laminated composite cantilever beam with three layers of height h, length L, width b under non-uniform temperature and moisture rising is shown in figure 1. It is assumed that height of layers is equal to each other. Temperature rising of bottom surface indicates as ΔT_B, whereas temperature rising of top surface indicates as ΔT_T. Moisture content rising of the bottom surface indicates as ΔC_B, whereas moisture content of the top surface indicates as ΔC_T. In figure 1, X-Y defines the initial coordinates and x-y defines the final coordinates.

The equivalent Young's modulus of kth layer in the X direction (E_x^k) as is used the following formulation (Vinson and Sierakowski 2002)

$$\frac{1}{E_x^k} = \frac{cos^4(\theta)}{E_{11}} + \left(\frac{1}{G_{12}} - \frac{2\nu_{12}}{E_{11}}\right) cos^2(\theta)\, sin^2(\theta) + \frac{sin^4(\theta)}{E_{22}}$$

where E_{11} and E_{22} indicate the Young's modulus in X and Y directions, respectively, G_{12} is the shear modulus, ν_{12} is Poisson's ratio θ is fiber orientation angle. Non-uniform temperature distribution for kth layer is expressed as follows;

$$\Delta T^k(Y) = \frac{\Delta T_B^k + \Delta T_T^k}{2} + \left(\frac{\Delta T_T^k - \Delta T_B^k}{h_k}\right) Y \quad -0.5h_k \le Y \le 0.5h_k$$

where, h_k indicates height of kth layer, ΔT_T^k and ΔT_B^k indicate temperature rising in top and bottom surfaces, respectively for the kth layer. In hygro-thermal effect, the Non-uniform moisture rising for kth layer is expressed as follows;

$$\Delta C^k(Y) = \frac{\Delta C_B^k + \Delta C_T^k}{2} + \left(\frac{\Delta C_T^k - \Delta C_B^k}{h_k}\right) Y \quad -0.5h_k \le Y \le 0.5h_k$$

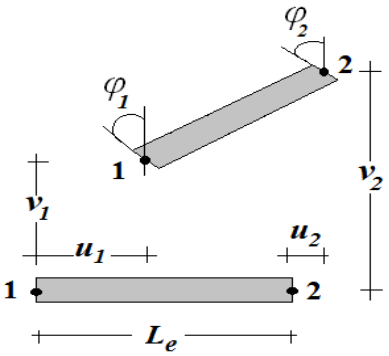

Fig. 2 Finite beam element model

The finite beam element with two nodes is used as shown in Fig. 2. The freedom degrees of the each node are horizontal displacement u, vertical displacement v and the rotation φ.

In the nonlinear kinematic formulations, the total Lagrangian (TL) model is used with the finite element formulations based on the first shear beam theory. In the TL kinematic model, the final coordinates of any point of the beam at the final configuration (x,y) are as follows

$$x = X + u - Y sin\varphi \tag{1}$$

$$y = v + Y cos\varphi \tag{2}$$

The differential arc length ds-displacement relations are given as follows

$$ds = \sqrt{(1+u')^2 + (1+v')^2}\, dX \tag{3}$$

$$1 + u' = \frac{L\, cos\varphi}{L_i}$$
$$v' = \frac{L\, sin\varphi}{L_i}, \qquad s' = \frac{L}{L_i} \tag{4}$$

The Green-Lagrange strain-displacement relation with hgyro-thermal effect is given as follows;

$$\{\epsilon\} = \begin{Bmatrix}\epsilon_{XX}\\ 2\epsilon_{XY}\end{Bmatrix} = \begin{Bmatrix}\epsilon_{XX}\\ \gamma\end{Bmatrix} = \begin{Bmatrix}(1+u')cos\varphi + v'\, sin\varphi - 1 - Y\kappa - \alpha_{11}\Delta T - \beta_{11}\Delta C\\ (1+u')sin\varphi + v'\, sin\varphi\end{Bmatrix} \tag{5a}$$

$$\{\epsilon\} = \begin{Bmatrix}\epsilon_{XX}\\ \gamma\end{Bmatrix} = \begin{Bmatrix}e - Y\kappa - \alpha_{11}\Delta T - \beta_{11}\Delta C\\ \gamma\end{Bmatrix} \tag{5b}$$

where ϵ_{XX}, γ, $\kappa = \varphi'$ are the axial strain, the shear strain and the curvature, respectively. α_{11} and β_{11} indicate the thermal expansion and moisture expansion coefficients in the longitudinal direction, respectively. In equation (5), $e = (1+u')cos\varphi + v'\, sin\varphi - 1$. Each node of the finite element has three freedom degrees and the displacement vector $\{\boldsymbol{u}\}^{(e)}$ for a finite element is given as follows;

$$\{u\}^{(e)} = [\, u_1,\, v_1,\, \varphi_1,\, u_2,\, v_2,\, \varphi_2\,]^T \tag{6}$$

The displacement fields ($\{\boldsymbol{u}\}^{(e)}$) of a finite beam element are given in terms of the node displacements as follows

$$u_x^{(e)} = N_1^{(u)}\, u_1 + N_2^{(u)}\, u_2 \tag{7}$$

$$u_y^{(e)} = N_1^{(v)} v_1 + N_2^{(v)} \varphi_1 + N_3^{(v)} v_2 + N_4^{(v)} \varphi_2 \tag{8}$$

$$\varphi^{(e)} = N_1^{(\varphi)} v_1 + N_2^{(\varphi)} \varphi_1 + N_3^{(\varphi)} v_2 + N_4^{(\varphi)} \varphi_2 \tag{9}$$

where $N_{\mathrm{i}}^{(u)}$, $N_{\mathrm{i}}^{(v)}$ and $N_{\mathrm{i}}^{(\varphi)}$ are the interpolation functions for axial displacement, vertical displacement and rotation, respectively. The strain-displacement relation is presented with the nodal displacements in matrix form;

$$\{\epsilon\} = [D]\{u\}^{(e)} \tag{10}$$

where $[D]$ is a differential operator matrix which related between the strain and the displacement vector. With using linear interpolation functions, the differential operator is given as follows:

$$[D] = \frac{1}{L_i}\begin{bmatrix} -cos\varphi & -sin\varphi & \gamma\, N_2^{(\varphi)} L_i & cos\varphi & sin\varphi & \gamma\, N_4^{(\varphi)} L_i \\ sin\varphi & -cos\varphi & -N_2^{(\varphi)}(1+e)L_i & -sin\varphi & cos\varphi & -N_4^{(\varphi)}(1+e)L_i \\ 0 & 0 & -1 & 0 & 0 & 1 \end{bmatrix} \tag{11}$$

The second Piola-Kirchhoff stresses-the Green-Lagrange strain relation with hgyro-thermal effect is given for linear elastic material in *k*th layer as follows;

$$\{\boldsymbol{S}\} = \begin{Bmatrix} S_{XX} \\ S_{XY} \end{Bmatrix} = \begin{bmatrix} E_x^k & 0 \\ 0 & G_x^k \end{bmatrix} \begin{Bmatrix} e - Y\kappa - \alpha_{11}\Delta T - \beta_{11}\Delta C \\ \gamma \end{Bmatrix} = [C]\{\epsilon\}, \quad [C] = \begin{bmatrix} E_x^k & 0 \\ 0 & G_x^k \end{bmatrix} \tag{12}$$

where α_{11} and β_{11} indicate the thermal expansion and moisture expansion coefficients in the longitudinal direction, respectively. G_x^k indicates equivalent shear modulus of *k*th layer. S_{XX} and S_{XY} indicate the second Piola-Kirchhoff stresses axial and shear components, respectively. Substituting equations (10) into equation (12), the constitutive relation is expressed as follows

$$\{\boldsymbol{S}\} = [C][D]\{u\}^{(e)} \tag{13}$$

The virtual work equation of the beam element based on the TL approach with neglecting the body forces is given as follows;

$$\int_V (s_{XX}\delta\varepsilon_{XX} + s_{XY}\delta\gamma)dV - \int_0 (r_X\delta u + r_Y\delta v)dS = 0 \tag{14a}$$

$$\int_V \{\boldsymbol{S}\}\{\delta\epsilon\}dV - \int_S \{\delta u^{(e)}\}^T [N]^T \begin{Bmatrix} r_X \\ r_Y \end{Bmatrix} dS = 0 \tag{14b}$$

where r_X and r_Y are the boundary forces in the *X* and *Y* directions respectively. *V* indicates the volume of the body. Substituting equations (13) and (10) into equation (14b) and applying the variational process, the virtual work equation is expressed as follows;

$$\int_V \left([C][D]\{u\}^{(e)}\right)\left(\frac{\partial[D]}{\partial u}\{\delta u\}^{(e)} + [D]\{\delta u\}^{(e)}\right) dV - \int_0^{L_e} \{\delta u^{(e)}\}^T [N]^T \begin{Bmatrix} r_X \\ r_Y \end{Bmatrix} dX \tag{15a}$$

$$\{\delta u\}^{(e)}\left(\int_V \left(\frac{\partial[D]^T}{\partial u}[C][D] + [D]^T[C][D]\right)\{u\}^{(e)}dV - \int_0^{L_e}[N]^T \begin{Bmatrix} r_X \\ r_Y \end{Bmatrix} dX\right) = 0 \tag{15b}$$

After integration process and the regulation of the equation (15b), the equation of motion is expressed as follows

$$\{\delta u\}^{(e)}\left(\int_0^{L_e}\left(\frac{\partial[D]^T}{\partial u}[C][D]A + [D]^T[C][D]A\right)dX - \int_0^{L_e}[N]^T \begin{Bmatrix} r_X \\ r_Y \end{Bmatrix} dX\right) = 0 \tag{16}$$

In equation (16), $\{u\}^{(e)}$ is the displacement vector. The element tangent stiffness matrix is presented as follows

$$\boldsymbol{K}_T = \boldsymbol{K}_M + \boldsymbol{K}_G \tag{17}$$

where $\boldsymbol{K}_G$ and $\boldsymbol{K}_M$ are the geometric and material stiffness matrixes, respectively

$$\boldsymbol{K}_M = \int_0^{L_e} [D]^T[C][D]A\, dX \tag{18}$$

$$\boldsymbol{K}_G = \int_0^{L_e} \frac{\partial[D]^T}{\partial u}[C][D]A\, dX \tag{19}$$

The load vector F is given as follows

$$\boldsymbol{F} = \int_0^{L_e} [N]^T \begin{Bmatrix} r_X \\ r_Y \end{Bmatrix} dX \tag{20}$$

In the nonlinear finite element solution, Newton-Raphson iteration procedure is considered. In solution procedure, the load is divided by an appropriate number with the small-step incremental. For n+1 st load increment and i th iteration, the increment displacement vector is given as follows;

$$d\boldsymbol{u}_n^i = \left(\boldsymbol{K}_T^i\right)^{-1}\boldsymbol{F}_{n+1}^i \tag{21}$$

where $\boldsymbol{K}_T^i$, $d\boldsymbol{u}_n^i$ and $\boldsymbol{F}_{n+1}^i$ are the tangent stiffness matrix, the increment displacement vector and the load vector, respectively for i th iteration and n+1 st load increment. The iteration tolerance form is selected in the Euclidean norm as follows;

$$\sqrt{\frac{[(d\boldsymbol{u}_n^{i+1} - d\boldsymbol{u}_n^i)^T(d\boldsymbol{u}_n^{i+1} - d\boldsymbol{u}_n^i)]^2}{[(d\boldsymbol{u}_n^{i+1})^T(d\boldsymbol{u}_n^{i+1})]^2}} \le \xi_{tol} \tag{22}$$

The updated displacement vector after the end of the i th iteration and n+1 st load increment is given as follows;

$$\boldsymbol{u}_{n+1}^{i+1} = \boldsymbol{u}_{n+1}^{i} + d\boldsymbol{u}_{n+1}^{i} = \boldsymbol{u}_{n} + \Delta\boldsymbol{u}_{n}^{i} \quad (23)$$

where

$$\Delta\boldsymbol{u}_{n}^{i} = \sum_{k=1}^{i} d\boldsymbol{u}_{n}^{k} \quad (24)$$

The dimensionless quantities can be expressed as,

$$T_R = \frac{\Delta T_T}{\Delta T_B}\ ,\ C_R = \frac{\Delta C_T}{\Delta C_B},\ \lambda = \delta^2 \alpha_{11}\, \Delta T_B\ ,$$
$$c\lambda = \delta^3 \beta_{11}\, \Delta C_B, \quad (25)$$
$$\delta = {}^{L}/_{h}\ ,\ \bar{v} = {}^{v}/_{L}\ ,\bar{X} = {}^{X}/_{L}\ ,\ \bar{Y} = {}^{Y}/_{L}$$

where T_R indicates temperature ratio of top and bottom surfaces, C_R indicates moisture ratio of top and bottom surfaces, λ is the dimensionless temperature rising, $c\lambda$ is the dimensionless moisture rising, δ is the ratio of length and height, $\bar{v}$ is the dimensionless vertical displacement, $\bar{X}$ and $\bar{Y}$ are dimensionless coordinates in the X and Y directions, respectively. If $T_R = 1$ and $C_R = 1$, hygrothermal rising becomes uniform distribution, otherwise it becomes non-uniform distribution.

3. Numerical results

In this section, the hygrothermal nonlinear bending deflections and displacement configurations of the laminated cantilever beam are calculated for different fiber orientation angles, the stacking sequence of laminates, temperature rising values and moisture rising values. In iteration process, moisture and temperature values are divided by a suitable number in compliance with the size values.

The laminated beam is established by of Graphite/Epoxy (T300/5208), and its material properties are as follows (Pipes *et al.* (1976)); E_{01}=143 GPa, E_{02}=10,1 GPa, G_{012}=4,14 GPa, α_{011}=1,1x10^{-6} $1/{}^{0}C$, α_{022}= 25,2x10^{-6} $1/{}^{0}C$, β_{11}=0.0010 *wt %*$^{-1}$, β_{22}=0.00667 *wt %*$^{-1}$. The height of three layers is equal to each other. The geometry values of the beam are selected as: b = 0.2 m, h = 0.2 m and the length L is varied according to the δ ratio in the numerical results.

In order to obtain number of the finite elements, the convergence study is employed in figure 3. The convergence is calculated for he nonlinear maximum displacements (at free end) for $\lambda = 2$, $c\lambda = 5$, $T_R = 0.1$, $C_R = 0.1, \delta = 20$, *30/0/30* stacking sequence. It is seen from fig. 3 that the nonlinear maximum displacements converge perfectly after the finite element as 100. In the numerical results, the number of the finite elements is taken as 100.

In order to verify the present formulation, the results obtained from the present study are compared with those obtained using ANSYS Workbench 14 (2012) which a finite element analysis program. In the comparison study, the nonlinear deflections of the free end of beam are calculated for $\Delta T_B = 50\,K$, 30 ^{0}C, $\Delta T_T = 20$ ^{0}C, $C_T = \%0\ wt$, $C_B = \%0\ wt$ for different fiber orientation angles and the stacking sequence of laminates in table 1. The beam is modeled as 3D solid in ANSYS. The comparison study shows in table 1 that the results of present study are very close to those of ANSYS Workbench 14.

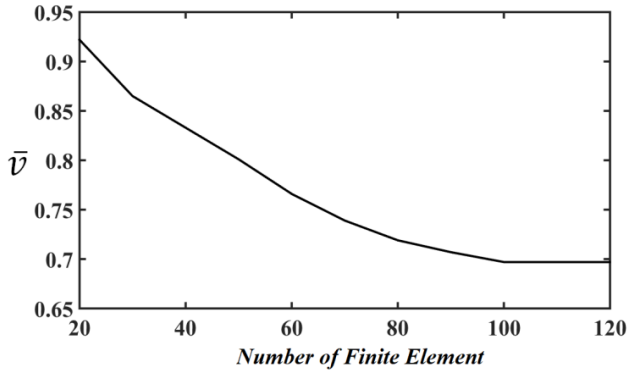

Fig. 3 Convergence analysis for nonlinear hygrothermal vertical displacements of the laminated beam

Table 1 Comparison study: Nonlinear deflections of the free end of laminated beam for different temperature values

		ΔT_B		
		100 ^{0}C	200 ^{0}C	400 ^{0}C
0/30/0	Present	0.0169 m	0.0381 m	0.0805 m
	ANSYS Workbench 14	0.0173 m	0.0386 m	0.0811 m
0/60/0	Present	0.0172 m	0.0388 m	0.0818 m
	ANSYS Workbench 14	0.0176 m	0.0393 m	0.0823 m
0/90/0	Present	0.2504 m	0.5616 m	1.1688 m
	ANSYS Workbench 14	0.2509 m	0.5624 m	1.1697 m

In figure 4, the temperature-nonlinear displacement curves are presented for different dimensionless moisture content values ($c\lambda$) for different stacking sequences for $T_R = 0.1$, $C_R = 0.1, \delta = 20$ under non-uniform hygro-temperature rising. In figure 4, the nonlinear maximum displacements (at free end) are calculated for the stacking sequences *0/0/0*, *30/0/30*, *45/0/45*, *0/90/0*.

It is seen from figure 4 that increasing moisture content, nonlinear displacements increase significantly. The difference between among the moisture content values increases with increasing the fiber orientation angles to 0° from 45°. At the stacking sequence *45/0/45*, the moisture effects reach highest level. In *0/0/0* and *0/90/0*, the moisture less effects the laminated beam. It shows that the stacking sequence is very effective in hgyro-thermal nonlinear responses of laminated composite beams. It can be concluded that effects of the moisture can be decreased by choosing of suitable stacking sequence laminas.

In figures 5 and 6, effects of fiber orientation angles on dimensionless maximum nonlinear displacements are plotted for the stacking sequences [*0/θ/0*] and [*θ/0/θ*], respectively, for different dimensionless temperature values (λ) and moisture content values ($c\lambda$). In figures 5 and 6 are obtained for non-uniform hygro-temperature rising for $T_R = 0.1$, $C_R = 0.1$, $\delta = 20$.

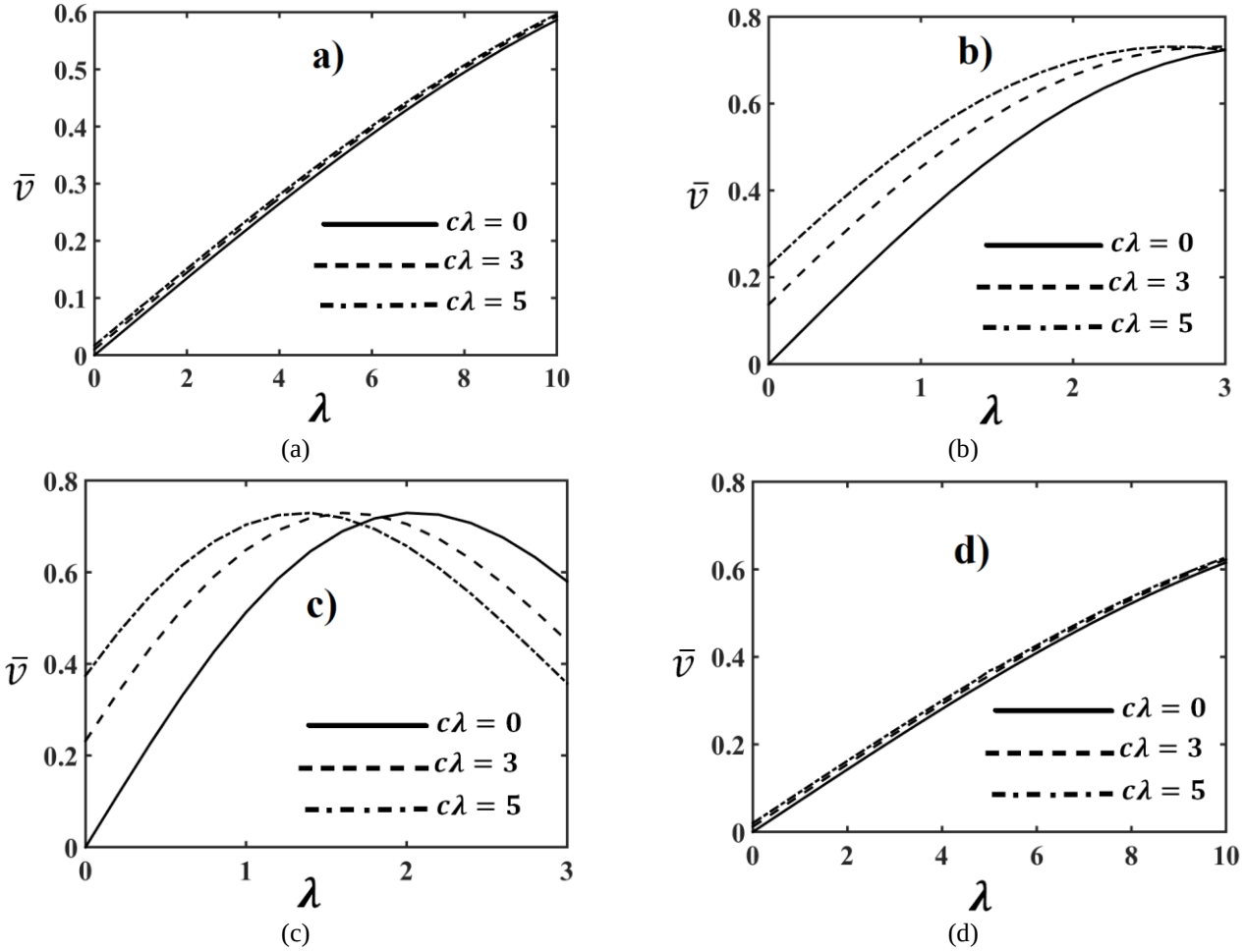

Fig. 4 Dimensionless temperature rising- dimensionless nonlinear vertical displacements curves for different dimensionless moisture content values with the different stacking sequences (a) for [*0/0/0*] (b) for [*30/0/30*], (c) for [*45/0/45*] and(d) for [*0/90/0*]

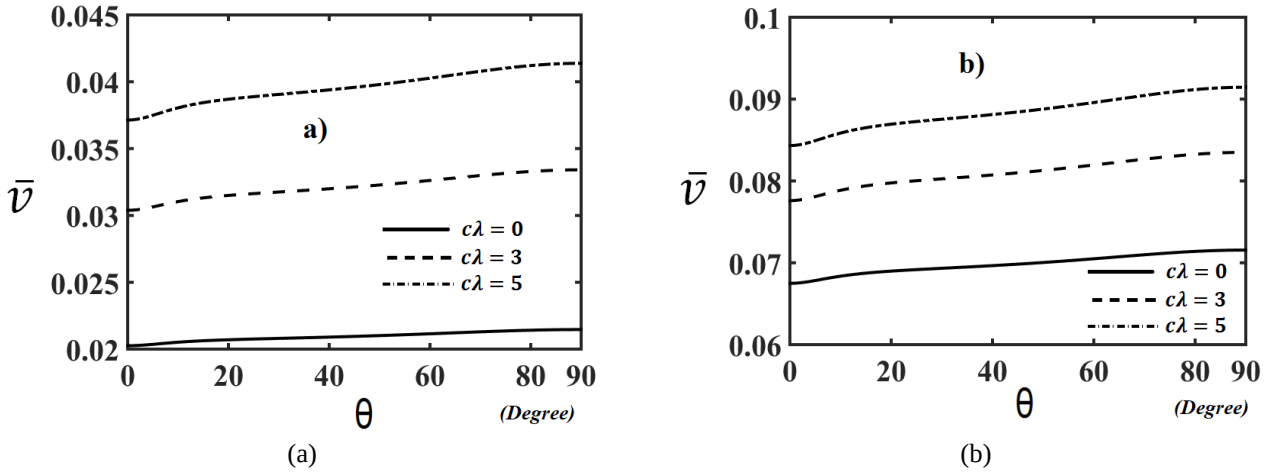

Fig. 5 The relationship between fiber orientation angles and nonlinear maximum vertical deflections for [*0/θ/0*] for different dimensionless moisture and temperature values (a) for $\lambda = 0.3$ and (b) for $\lambda = 1$

Figures 5 and 6 display that hygro-thermal displacements rise considerably with rising in fiber orientation angles. This is because that the strength of composite laminated beam is the highest level at fiber orientation angle θ=0° according to equation 1.

The effects of moisture on the nonlinear displacements of laminated beam in [*θ/0/θ*] stacking sequence are bigger than those of [*0/θ/0*]'s stacking sequence. The nonlinear deflections of [*θ/0/θ*] stacking sequence are bigger than nonlinear deflections of [*0/θ/0*]'s.

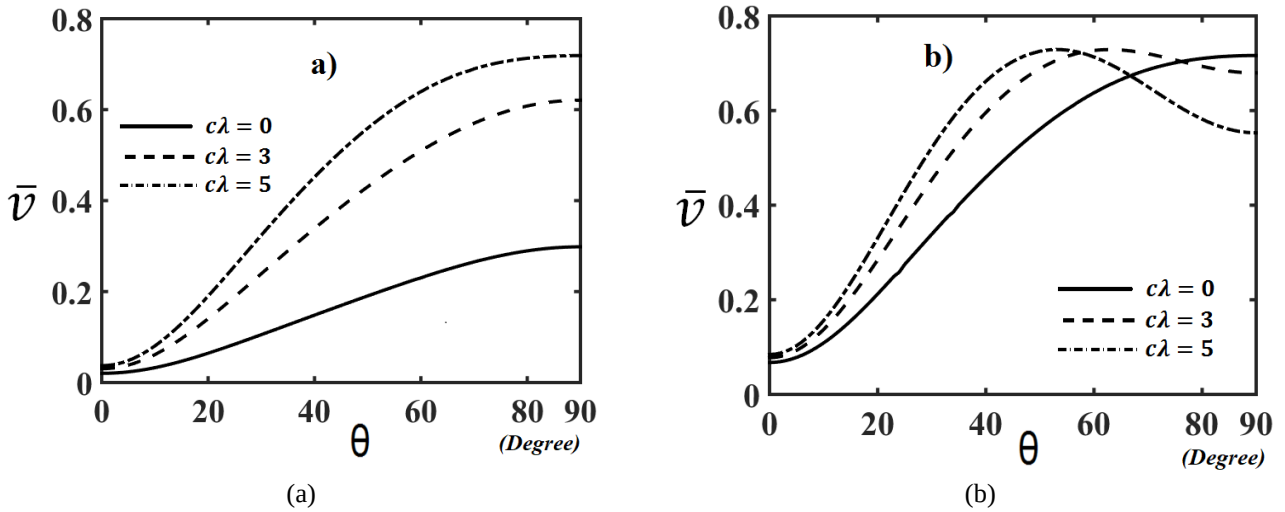

(a) (b)

Fig. 6 The relationship between fiber orientation angles and nonlinear maximum vertical deflections for [$\theta/0/\theta$] for different dimensionless moisture and temperature values (a) for $\lambda = 0.3$ and (b) for $\lambda = 1$

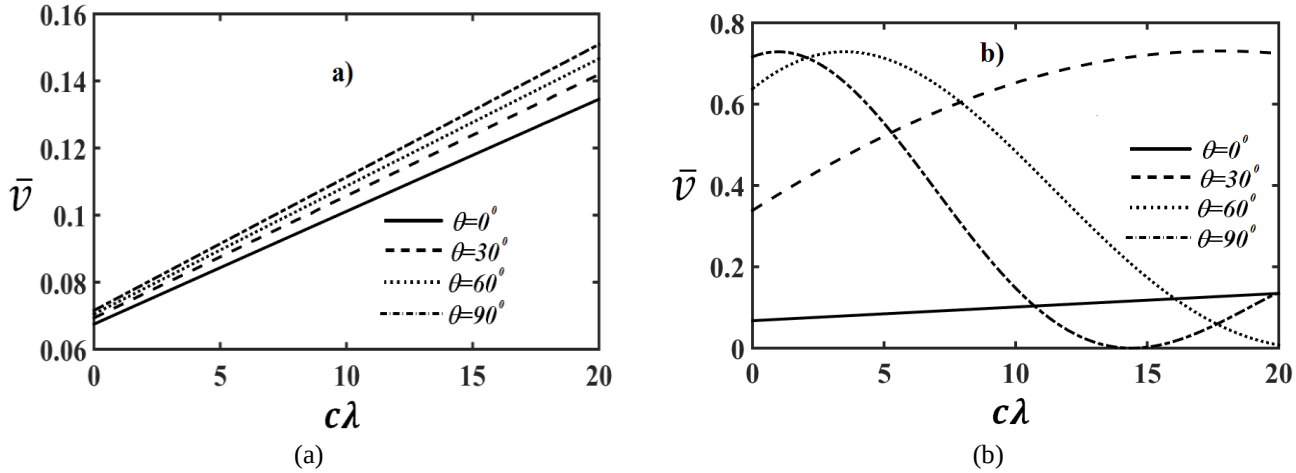

(a) (b)

Fig. 7 The relationship between dimensionless moisture content ($c\lambda$) and nonlinear maximum vertical deflections for different fiber orientation values in and stacking sequences a) for [$0/\theta/0$] and b) for [$\theta/0/\theta$]

In another results of figures 5 and 6 that the difference between the moisture content values in nonlinear deflections of laminated composite beams increases significantly with rising temperature in [$\theta/0/\theta$] stacking sequence. However, this case is not valid in [$0/\theta/0$] stacking sequence. In [$\theta/0/\theta$] stacking sequence, both moisture and temperature are very effective in the nonlinear behaviour of laminated beam. Another result of figures 4 and 5 that the moisture is very effective in the lower values of temperature rising.

With increasing the temperature, the effects of moisture on the nonlinear behavior of laminated beams decrease significantly. Especially, this situation is seen more clearly in results of [$\theta/0/\theta$] stacking sequence. It shows that stacking sequence and temperature have important role on effects of moisture in laminated composite beams.

Figure 7 highlights the moisture-nonlinear displacement curves are displayed in dimensionless quantities for fiber orientation values in [$0/\theta/0$] and [$\theta/0/\theta$] stacking sequences for $\lambda = 1,\ T_R = 0.1,\ C_R = 0.1, \delta = 20$.

As seen from figure 7 that increasing the moisture yields to increase the difference among of fiber orientation angles. However, this difference is very big significantly in [$\theta/0/\theta$] in contrast with [$0/\theta/0$]. With change in stacking sequence of laminas, the effects of moisture differ considerably. In [$0/\theta/0$] stacking sequence, nonlinear hygrothermal displacements increase monotonically with increasing of θ. However, nonlinear hygrothermal displacements completely differ with increasing θ in [$\theta/0/\theta$] stacking sequence. In higher moisture content, there are significant differences among of fiber orientation angles in [$\theta/0/\theta$] in contrast with [$0/\theta/0$].

Figures 8 and 9 display effect of moisture content values on the nonlinear hgyrothermal deflected shape of the laminated beam for fiber orientation values in [$0/\theta/0$] and [$\theta/0/\theta$] stacking sequences for $\lambda = 1.5,\ T_R = 0.1,\ C_R = 0.1,\ \delta$=20. Figures 7 and 8 show that although the values of temperature ($\lambda = 1.5$) is stable, hygrothermal nonlinear displacement configuration of laminated beam change considerably with increasing the moisture content. In [$\theta/0/\theta$], the moisture is more effective and cause to more

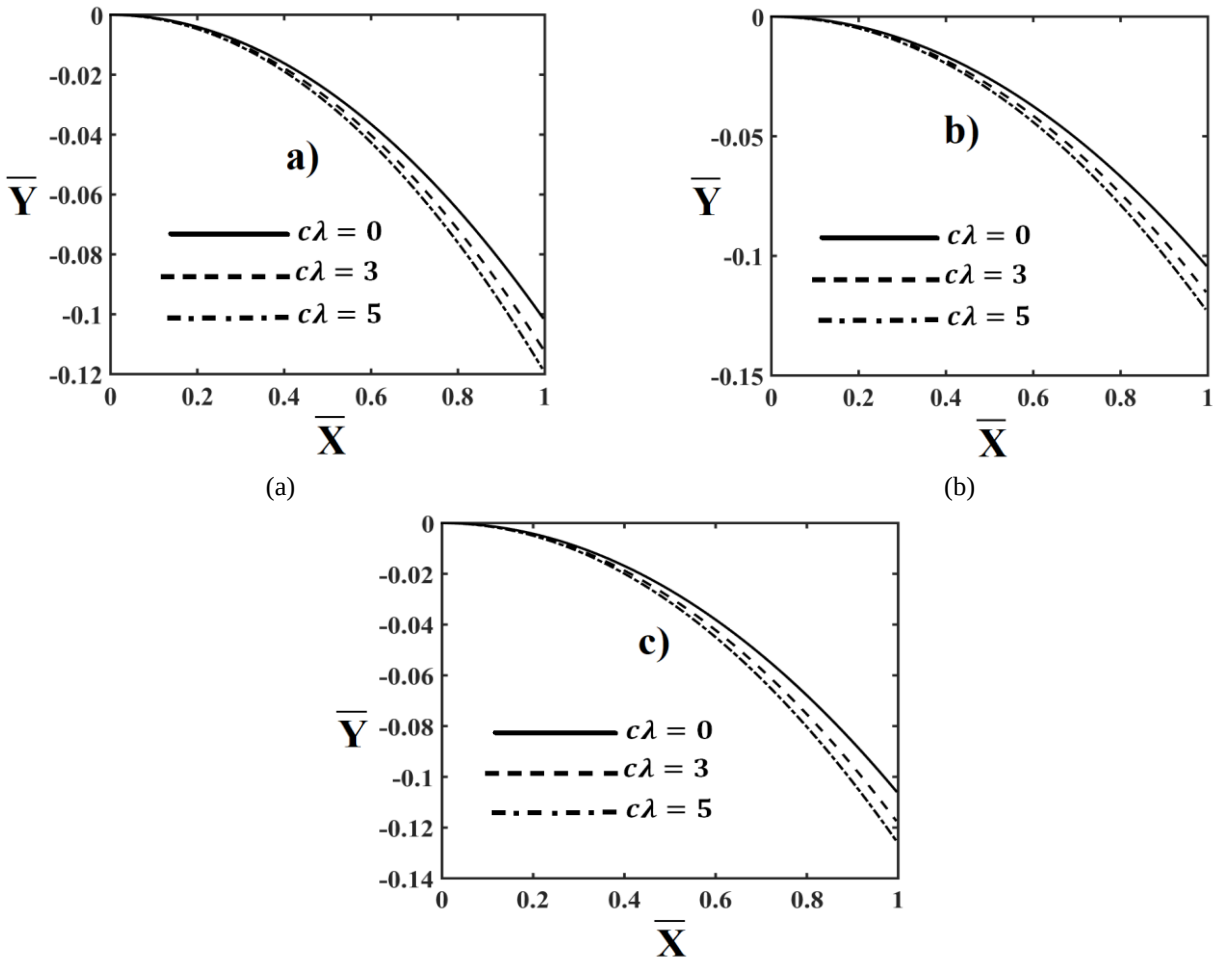

Fig. 8 Effects of the dimensionless moisture content values on nonlinear hgyro-thermal deflected shape of laminated beam in [*0/θ/0*] stacking sequence for different fiber orientation angles a) for [*0/0/0*], b) for [*0/30/0*] and c) for [*0/60/0*]

displacements. Increasing of θ yields to increase displacements of the laminated beam significantly. It shows that the moisture has important role on the nonlinear behavior of laminated composite beam.

4. Conclusions

Hygrothermal nonlinear displacements investigated for laminated composite beams within total Langragian nonlinearity approach. The influences of the moisture, temperature and parameters of the composite on the nonlinear displacements are investigated. It is concluded from the numerical results, the main results are as follows:

- The stacking sequence of laminas and the moisture play important role on hygrothermal nonlinear behaviour of composite laminated beams.
- Increasing moisture content yields to increasing hygrothermal nonlinear displacements significantly.
- With changing fiber orientation angles and stacking sequence, the effects of moisture on nonlinear hygrothermal behaviour of laminated composite beams change significantly.
- In smaller temperature values, the moisture is more effective on laminated composite beams.
- The effects of moisture can be decreased by suitable choice of stacking sequence laminas.

References

Akbaş, Ş.D. (2017a), "Thermal effects on the vibration of functionally graded deep beams with porosity", *J. Appl. Mech.*, **9**(05), https://doi.org/10.1142/S1758825117500764.

Akbaş, Ş.D. (2017b), "Nonlinear static analysis of functionally graded porous beams under thermal effect", *Coupl. Syst. Mech.*, **6**(4), 399-415. https://doi.org/10.12989/csm.2017.6.4.399.

Akbaş Ş.D. (2018a), "Post-buckling responses of a laminated composite beam", *Steel Compos. Struct.*, **26**(6), 733-743. https://doi.org/10.12989/scs.2018.26.6.733.

Akbaş Ş.D. (2018b), "Geometrically nonlinear analysis of a laminated composite beam", *Struct. Eng. Mech.*, **66**(1), 27-36. https://doi.org/10.12989/sem.2018.66.1.027.

Akbaş Ş.D. (2018c), "Thermal post-buckling analysis of a laminated composite beam", *Struct. Eng. Mech.*, **67**(4), 337-346. https://doi.org/10.12989/sem.2018.67.4.337.

Akbaş Ş.D. (2018d), "Large deflection analysis of a fiber

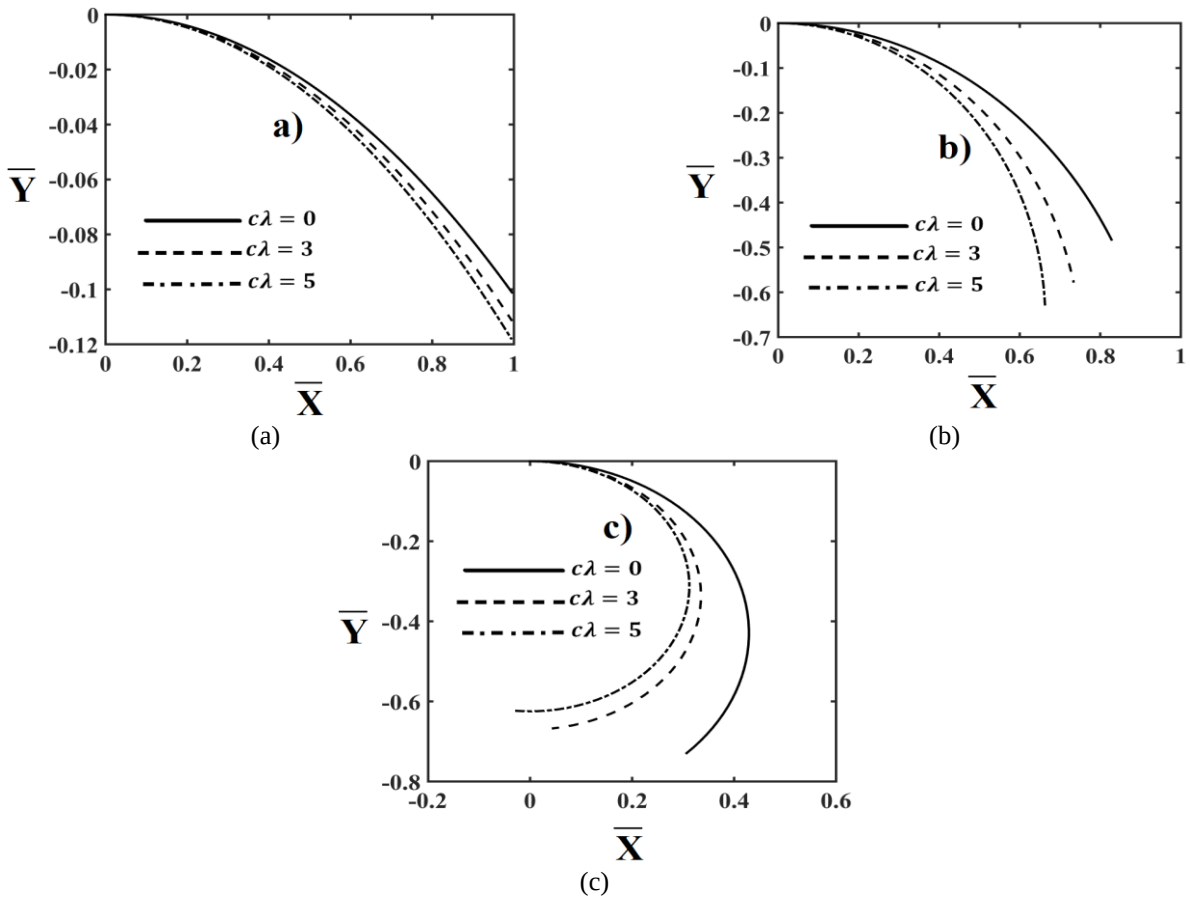

Fig. 9 Effects of the dimensionless moisture content values on nonlinear hgyrothermal deflected shape of laminated beam in [$\theta/0/\theta$] stacking sequence for different fiber orientation angles a) for [*0/0/0*], b) for [*30/0/30*] and c) for [*60/0/60*]

reinforced composite beam", *Steel Compos. Struct.*, **27**(5), 567-576. https://doi.org/10.12989/scs.2018.27.5.567.

Akbaş, Ş.D. (2019a), "Hygrothermal Post-Buckling Analysis of Laminated Composite", *J. Appl. Mech.*, **11**(1). https://doi.org/10.1142/S1758825119500091.

Akbaş, Ş.D. (2019b), "Post-Buckling Analysis of a Fiber Reinforced Composite Beam with Crack", *Eng. Fracture Mech.*, **212**(1), 70-80. https://doi.org/10.1016/j.engfracmech.2019.03.007.

Akbaş, Ş.D. (2019c), "Nonlinear Behavior of Fiber Reinforced Cracked Composite Beams", *Steel Compos. Struct.*, **30**(4), 327-336. https://doi.org/10.12989/scs.2019.30.4.327.

Akbaş, Ş.D. (2019d), "Hygro-Thermal Nonlinear Analysis of a Functionally Graded Beam", *J. Appl. Comput. Mech.*, **5**(2), 477-485.

Biswal, M., Sahu, S. K., Asha, A.V. and Nanda, N. (2016), "Hygrothermal effects on buckling of composite shell-experimental and FEM results", *Steel Compos. Struct.*, **22**(6), 1445-1463. http://dx.doi.org/10.12989/scs.2016.22.6.1445.

Bouazza, M, Amara, K, Zidour,M, Tounsi ,A, Adda-Bedia, E.A., (2014), "Hygrothermal effects on the postbuckling response of composite beams", *Am. J. Mater. Res.*, **1**(2): 35-43.

Cardoso, JB., Benedito, N.M. and Valido, A.J. (2009), "Finite element analysis of thin-walled composite laminated beams with geometrically nonlinear behavior including warping deformation", *Thin Wall. Struct.*, 47(11), 1363-1372. https://doi.org/10.1016/j.tws.2009.03.002.

Ebrahimi, F. and Hosseini, S.H.S. (2018), "Surface effects on nonlinear dynamics of NEMS consisting of double-layered viscoelastic nanoplates", *Struct. Eng. Mech.*, **65**(6), 645-656. https://doi.org/10.1140/epjp/i2017-11400-6.

Farokhi, H., Ghayesh, M. H., Gholipour, A. and Hussain, S. (2017), "Motion characteristics of bilayered extensible Timoshenko microbeams", *J. Eng. Sci.*, **112**, 1-17. https://doi.org/10.1016/j.ijengsci.2016.09.007.

Gayen, D. and Roy, T. (2013) "Hygro-thermal effects on stress analysis of tapered laminated composite beam", *J. Compos. Mater.*, **3**(3), 46-55. https://doi.org/10.5923/j.cmaterials.20130303.02.

Ghayesh, M. H., Yourdkhani, M., Balar, S. and Reid, T. (2010), "Vibrations and stability of axially traveling laminated beams", *Appl. Math. Comput.*, **217**(2), 545-556. https://doi.org/10.1016/j.amc.2010.05.088.

Ghayesh, M. H., Farokhi, H. and Gholipour, A. (2017), "Vibration analysis of geometrically imperfect three-layered shear-deformable microbeams", *J. Mech. Sci.*, **122**, 370-383. https://doi.org/10.1016/j.ijmecsci.2017.01.001.

Ghayesh, M. H. (2018), "Nonlinear vibration analysis of axially functionally graded shear-deformable tapered beams", *Appl. Math. Modell.*, **59**, 583-596. https://doi.org/10.1016/j.apm.2018.02.017.

Gholami, R., Ansari, R. and Gholami, Y. (2017), "Nonlinear resonant dynamics of geometrically imperfect higher-order shear deformable functionally graded carbon-nanotube reinforced composite beams", *Compos. Struct.*, **174**, 45-58. https://doi.org/10.1016/j.compstruct.2017.04.042.

Joshan, Y.S., Grover, N. and Singh, B.N. (2017), "A new non-polynomial four variable shear deformation theory in axiomatic formulation for hygro-thermo-mechanical analysis of laminated composite plates", *Compos. Struct.*, **182**, 685-693. https://doi.org/10.1016/j.compstruct.2017.09.029.

Kazemirad, S., Ghayesh, M. H. and Amabili, M. (2013), "Thermo-mechanical nonlinear dynamics of a buckled axially moving

beam", *Arch. Appl. Mech.*, **83**(1), 25-42. https://doi.org/10.1007/s00419-012-0630-8.

Li, Z.M. and Qiao, P. (2015), "Thermal postbuckling analysis of anisotropic laminated beams with different boundary conditions resting on two-parameter elastic foundations", *Europe. J. Mech. A Solid*, **54**, 30-43. https://doi.org/10.1016/j.euromechsol.2015.06.001.

Pipes, R.B., Vinson, J.R. and Chou, T.W. (1976), "On the hygrothermal response of laminated composite systems," *J. Compos. Mater.*, **10**(2), 129-148. https://doi.org/10.1177/002199837601000203.

Sahu, S.K., Rath, M.K. and Sahoo, R. (2012), "Parametric instability of laminated composite doubly curved shell panels subjected to hygrothermal environment", *Adv. Mater. Res.*, **383**, 3212-3216. https://doi.org/10.4028/www.scientific.net/AMR.383-390.3212.

Vinson, J.R. and Sierakowski, R.L. (2002), *The Behavior of Structures Composed of Composite Materials*, Springer, Germany.

Wang, H., Chen, C.S. and Fung, C.P. (2015), "Hygrothermal effects on the vibration and stability of an initially stressed laminated plate", *Struct. Eng. Mech.*, **56**(6), 1041-1061. https://doi.org/10.12989/sem.2015.56.6.1041.

Zenkour, A.M., Mashat, D.S. and Alghanmi, R.A. (2014), "Hygrothermal analysis of antisymmetric cross-ply laminates using a refined plate theory", *J. Mech. Mater. Des.*, **10**(2), 213-226. https://doi.org/10.1007/s10999-014-9242-5.

Zhan, Q.W., Fan, X.L. and Sun, Q. (2011), "Effects of hygrothermal environment on static properties of laminated composites with a circular open hole", *J. Solid Rocket Technol.,* **34**(6), 764-767.

CC